

# Study of Mechanical Properties of Solvent Cement Connection for PVC Pipes



Tao Wang and Shaowei Hu

**Abstract** For the mechanical properties of pipe joints, existing studies have mainly focused on flexible joints of ductile iron pipes and concrete pipes, and there is a lack of research on the mechanical properties of adhesive bonded joint of PVC pipes. By combining axial pullout prototype tests and numerical simulations using ABAQUS, this study investigated the effects of pipe diameter, socket gap, and loading rate on the axial mechanical properties of PVC pipe adhesive joints. Moreover, by building a buried PVC pipeline with 4 pipe sections, this study investigated the dynamic response of the adhesive bonded joint under different load amplitudes and different travel directions. The results showed that the seismic performance of the adhesive bonded joint is weak, and its axial pullout force is inversely proportional to the socket gap and proportional to the pipe diameter, while the loading rate has limited effect on it; under buried conditions, the longitudinal stress distribution at the top of the pipe is highly discontinuous, and the maximum stress in the socket is proportional to the traffic load amplitude, and the longitudinal travel direction is more likely to cause the failure damage of the buried PVC pipeline with adhesive bonded joint.

**Keywords** PVC pipes · Solvent cement connection · Parametric analysis · Numerical simulation · Adhesive bonded joint · Experiments

## 1 Introduction

Underground pipeline system is the infrastructure for transporting water in cities, and is the underground lifeline to ensure residents' life and production [1]. Polyvinyl chloride (PVC) pipes, as a national effort to promote the development of eco-friendly

---

T. Wang (✉)

Department School of Civil Engineering, Chongqing University, Chongqing 400045, China  
e-mail: [wangtaobenny@163.co](mailto:wangtaobenny@163.co)

S. Hu

Yellow River Laboratory, Zhengzhou University, Zhengzhou 450001, China  
e-mail: [hushao-wei@zzu.edu.cn](mailto:hushao-wei@zzu.edu.cn)

pipes, have the advantages of flexibility, low flow resistance, reliable sealing, and corrosion resistance [2]. Many studies have pointed out [1, 3–5] that the interface area of pipes is the weak part in the mechanical properties of buried pipelines and is more prone to damage during earthquakes, so it is crucial to effectively improve the mechanical properties of water pipeline interfaces.

Currently in the Chinese standard regarding PVC pipes [6, 7], the interface connections of PVC pipelines are mainly divided into two types of flexible connections and rigid connections. And rigid connection mainly includes solvent cement connection, flange connection and other connection methods, of which the most applied is the solvent cement connection (adhesive bonded joint, or adhesive interface), whose applicable range is less than 225 mm nominal diameter.

A major evaluation indicator for buried pipelines is seismic capacity, Chen et al. [8] concluded that the flexible interface has good seismic energy dissipation capability by conducting axial pull-out test on foot-rule cast iron pipeline; Han et al. [3] proposed the axial stiffness equation of socketed flexible interface by conducting axial pull-out test on ductile iron pipeline; Ren et al. [4] studied the damage form of flexible interface of ductile iron pipeline under eccentric stretching; Li et al. [9] obtained the hysteresis curves of flexible interfaces of ductile iron pipes under reciprocal loading and found that the magnitude of seismic capacity was positively correlated with the size of pipe diameter through tests; Zhong et al. [5] studied the bending performance of the flexible interface of ductile iron pipeline; Duan [10] studied the seismic performance of the socket interface of cast iron pipeline by bending test; Wang et al. [11, 12] investigated the mechanical response of flexible interfaces of buried concrete pipes under coupled traffic and operational loads through three-dimensional numerical simulations; Zhai et al. [13] studied the failure mode of the socket of PCCP pipes and found that the increase of joint gap is not conducive to socket joint protection; Chen et al. [14] compared the seepage resistance of flexible and rigid interfaces through the leakage test of concrete drainage pipes and found that flexible interfaces such as rubber rings have better impermeability; Zhang et al. [15] obtained the analysable solution of internal force and displacement of arbitrary cross-section of gas transmission pipeline under rainfall conditions; Wu et al. [16] established the calculation model and calculation method of vertical displacement of flexible interface pipeline under vertical load.

The above-mentioned studies in the field of buried pipes are more on the mechanical response of the interfaces of cast iron and concrete pipes, but rarely on the interfaces of PVC pipes, and mostly focus on the flexible interface as the connection form, lacking studies on the adhesive connection form.

In this study, based on the previous studies, the axial mechanical properties of PVC pipes with adhesive bonded joints under different pipe diameters, loading rates, and socket gaps by means of a three-dimensional solid numerical model established by ABAQUS software were investigated. Further, the three-dimensional solid model of the interaction between the road structure and the buried PVC pipeline with adhesive bonded joint of multiple pipe joints is established, and the mechanical response of the buried PVC pipeline with adhesive interface is studied by applying different traffic

load amplitudes and different travel directions. The results of this study will provide guidance for practical engineering.

## 2 Axial Mechanical Properties

The seismic data over the years show that the bending deformation of buried pipes caused by seismic wave propagation can be almost negligible compared to the axial deformation [3], so it is necessary to study the axial mechanical response of PVC pipes with adhesive bonded joints.

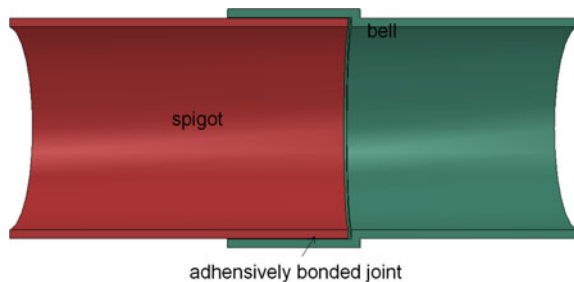
### 2.1 Finite Element Model

To investigate the mechanical response of the adhesive interface under different loading regimes, the 3D solid model of the adhesive bonded joint is established in ABAQUS as Fig. 1, which consists of three components: bell, spigot and adhesive layer [17, 18]. In this simulation, the end of the bell is fixed while the end of the spigot is loaded according to the displacement to simulate the pulling process of the adhesive interface.

The material of the PVC pipe composed of bell and spigot was set as an elastoplastic material, and the elastic modulus and Poisson's ratio were respectively set to 0.3 GPa and 0.35 [3], with C3D8R cell type and hourglass control.

The finite element model approach for the adhesive interface is mainly surface-based cohesive and using solid cells, among which the simulation results obtained by using the solid cell approach are more realistic and accurate compared to the former [19, 20]. For the above reasons, this study adopted the method of establishing solid cells for finite element simulation of PVC adhesive interfaces, and its intrinsic model is the BK composite mode under energy-based damage evolution [21–23]. The adhesive layer was processed using the COH3D8 cell type as shown in Fig. 2 in ABAQUS software, where the upper surface of the adhesive layer was designated as the top surface. Connect the outer wall of the spigot to the inner wall of the adhesive

**Fig. 1** Structure of solvent cement connection



layer and the inner wall of the bell to the outer wall of the adhesive layer using a Tie connection in ABAQUS.

At present, research on the performance of adhesive interface materials is mainly focused on the aerospace and chemical industry, and less research has been conducted on the adhesive layer used for PVC adhesive interfaces. The bonding properties of different base materials and adhesives are not consistent, to obtain the material parameters for characterizing the adhesive layer, the material property tests were carried out according to the standards [24–26], and the normal tensile test and shear test were performed as shown in Fig. 3. According to the stress–strain curve obtained from the test results, the values of the material parameters used in this paper are shown in Table 1.

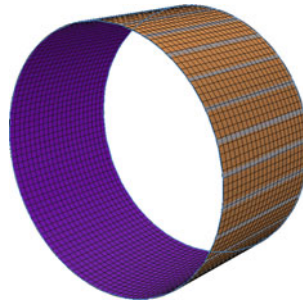


Fig. 2 Orientation of the adhesive layer mesh

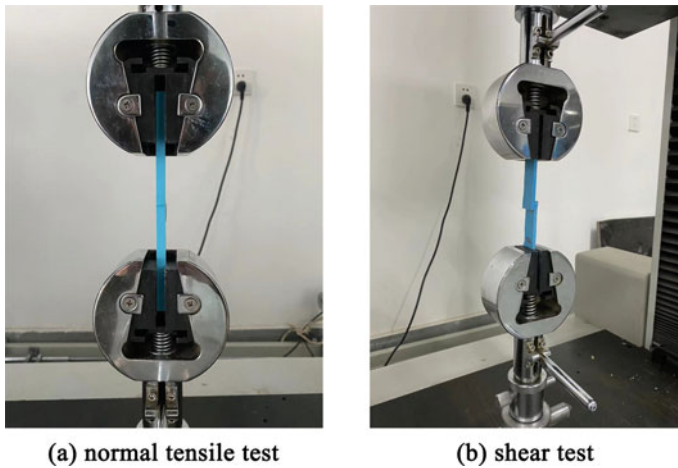


Fig. 3 Adhesive mechanical properties materiality test

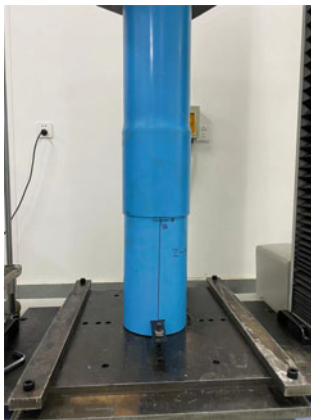
**Table 1** Parameters for characterizing adhesive materials in ABAQUS

$E_{nn}$	$E_{ss}$	$E_{tt}$	$\sigma_{nn}$	$\sigma_{ss}$	$\sigma_{tt}$	$G_{IC}$	$C_{IIC}$	$G_{IIIc}$
0.671	2.143	2.143	0.612	5.892	5.892	1.365	10.178	10.178

## 2.2 Results and Discussion

The response of the axial mechanics of the PVC pipe line was accessed by simulating the pulling process of adhesive bonded joint. To verify the accuracy of the numerical simulation and ensure the validity of the subsequent results, a proposed static test of the axial pullout of the adhesive interface is designed in this paper, and the test setup and procedure of this test are shown in Fig. 4 where bell and spigot of the pipeline were fixed at the two ends of the loading device respectively. A universal testing machine was used for displacement loading, and the axial pulling force and displacement of the specimen during the press-pulling process were collected by force and displacement sensors. The experimental results are compared with the results of the numerical simulation in Fig. 5, from which it can be seen that the results of the simulation are quite consistent with the experimental ones, which ensures that the finite element model used in this simulation is valid.

**Loading Rate.** The relationship between the measured axial pullout force and socket displacement (F-D curves) is shown in Fig. 6 when different loading rates (10 mm/s, 20 mm/s, 50 mm/s) were applied to a socket with DN200 and a socket gap of 1 mm. In Fig. 6, for PVC pipelines with adhesive bonded joints, increasing the pullout rate does not change the nominal stiffness of the interface to resist pullout, but can increase the maximum failure load to some extent, although the change was relatively small and its effect can be ignored in practical engineering applications. In the early pulling



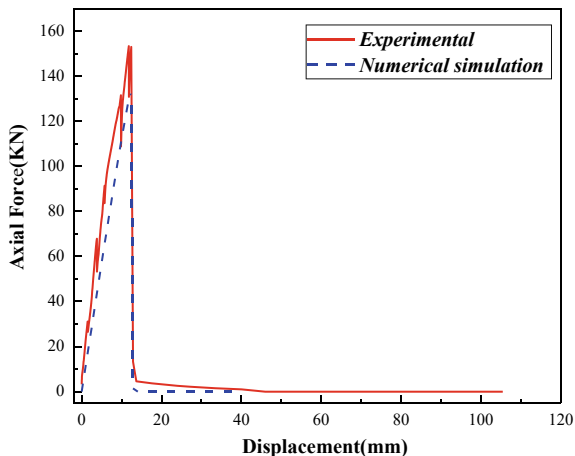
(a) Prototype test site



(b) The pipeline prepared for the test

**Fig. 4** Prototype test of PVC pipeline with solvent cement connection

**Fig. 5** Comparison of prototype test results and numerical simulation results for PVC pipelines with solvent cement connection



period, the adhesive interface in the axial pulling force basically maintained linear elasticity, when the ultimate load was reached, rapid tearing damage occurred and the interface collapsed. This explained that the change in velocity of seismic waves in earthquake was less influential in producing damage to the adhesive interface. Nevertheless, the PVC pipe with adhesive interface of DN200 failed by pull-out damage after 12 mm of socket displacement, which indicated that the resistance of interface to seismic damage is very weak and much lower than that of flexible interface. But compared to the flexible joint, DN200, socket gap of 1 mm adhesive bonded joint limited pullout force of about 250 kN, while the same specifications of the flexible joint limit pullout force were often only about 600 N, which makes the adhesive bonded joint has a much higher than the flexible interface stopping ability. Therefore, for the buried PVC pipeline with adhesive interface, it is not necessary to set up support piers along the laying direction, which will greatly save the project cost in the short and medium distance water transmission project with small diameter requirements.

**Pipe Diameter.** To study the effect of pipe diameter size on the mechanical properties of the interface, three nominal diameters of PVC pipes, DN200, DN160 and DN110, were taken for simulation in ABAQUS, and the obtained F-D curves are shown in Fig. 7.

From Fig. 7, for PVC pipelines with adhesive bonded joints, not only the maximum pullout force would increase significantly with the increase of pipe diameter, but also the nominal stiffness of the interface to resist pullout could be increased. Further, the maximum pullout force does not simply increase linearly with the increase in pipe diameter. The maximum pullout load per week increased with the increase of pipe diameter, which indicated that the increase of pipe diameter changes the mechanical mechanism of the adhesive interface. Since the bonding force of the adhesive interface comes from the cohesive force of the adhesive and the bonding force between the adhesive and the pipe wall, the increase of the pipe diameter did

**Fig. 6** Relationship between tensile force and interface displacement of PVC pipe socket with DN200 adhesive interfaces at different loading rates

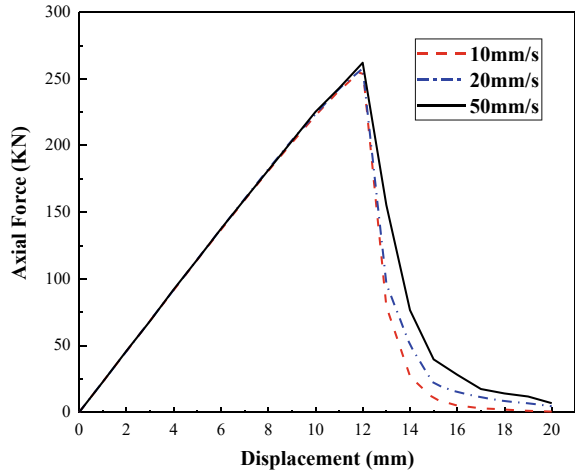
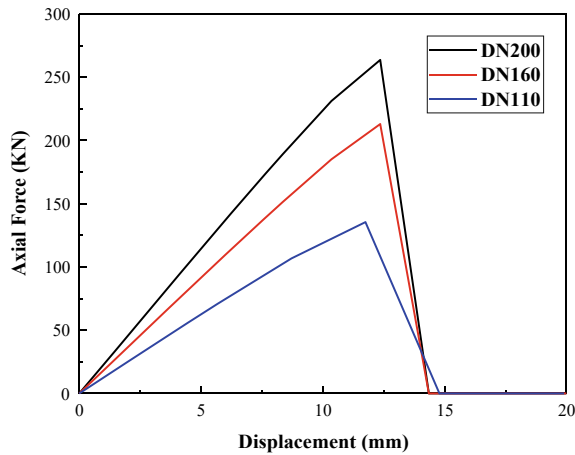


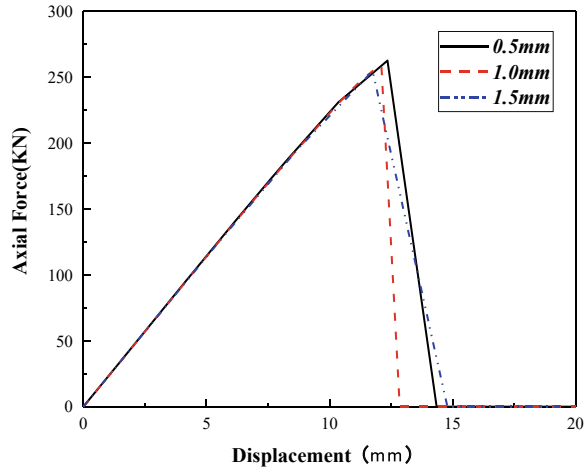
**Fig. 7** Relationship between pull-out force and interface displacement of PVC pipe socket for adhesive interfaces at different pipe diameters



not change the cohesive force of the adhesive, which indicated that the increase of the pipe diameter will increase the bonding force between the adhesive and the pipe wall and there was a size effect.

**Socket Gap.** In the assembly process, the socket gap of the adhesive interface will affect the bonding ability between the adhesive and the bonding interface, so the size of the socket gap is an important factor affecting the mechanical properties of joint. To investigate the effect of different gap sizes on the axial pullout force of the adhesive interface, different assembly gaps were set as variables in this section, and the F-D curve about axial mechanical response of the adhesive interface is shown in Fig. 8. As it can be seen from Fig. 8, for the adhesive interface, the increase of the socket gap did not change the magnitude of the nominal stiffness of the interface to

**Fig. 8** Relationship between pull-out force and interface displacement of PVC pipe socket for adhesive interfaces at different socket gap



resist pullout, while its maximum pullout force decreased with the increase of the socket gap, which led to the forward shift of the appearance of the maximum pullout force. Although increasing the socket gap means using more adhesive to bond bell and spigot, it reduced the tensile strength of the socket, so it was more economical and beneficial to avoid using adhesive interfaces with large socket gaps in the project. The increase of the socket gap did not change the adhesive mechanics of the adhesive interface, but only makes the bonding force between the adhesive and the pipe wall reduced, thus weakening the working ability of the adhesive interface.

### 3 Buried Pipeline Mechanical Properties

#### 3.1 Finite Element Model

The whole model consists of two major parts: the pipeline model and the road model. The pipeline model consisted of 4 sections of the same length connected to each other, and the two adjacent sections were connected by adhesive joints, each with an effective length of 2 m and a nominal diameter of DN 200. The material parameters of the PVC pipeline and adhesive joints were set as before. The overall model of the pipeline is shown in Fig. 9 (P1, P2, P3, P4 represent the 1st, 2nd, 3rd, 4th pipe sections, S1, S2, S3 represent the 1st, 2nd, 3rd adhesive bonded joint).

The road model consisted of three parts: road surface, roadbed and sand subcrust, and the overall model size is 7 m × 8 m × 8 m. The thickness of the road surface was 0.25 m and adopted the linear elastic principal structure. The thicknesses of roadbed and sand subcrust were 6.75 m and 0.25 m respectively, and the width of sand sub-crust was 0.60 m. Both the roadbed and sand subcrust used the Moore



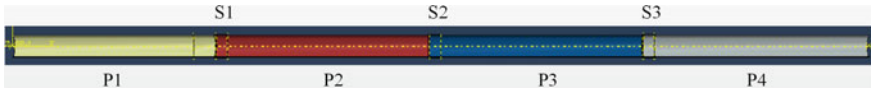


**Fig. 9** Modeling of pipeline entities

Coulomb elastoplastic principal structure model. The relevant material parameters are shown in Table 2 [11, 12, 27], and the overall mesh is divided as shown in Fig. 10. To simulate the boundary conditions of the buried pipeline more realistically, the displacement degrees of freedom of the bottom 3 directions and the displacement degrees of freedom of the 4 lateral normal directions are constrained in the road model.

**Table 2** Material parameters of road structures

Material	Density $\rho$ / ( $\text{kg}\cdot\text{m}^{-3}$ )	Elastic modulus $E$ / (MPa)	Poisson's ratio $\mu$	Cohesive force $c$ /(kPa)	Angle of internal friction $\varphi$ /( $^{\circ}$ )
Road surface	2400	240	0.3	–	–
Roadbed	2000	15	0.26	20	25.4
Sand subcrust	2200	1400	0.25	$1 \times 10^{-3}$	37

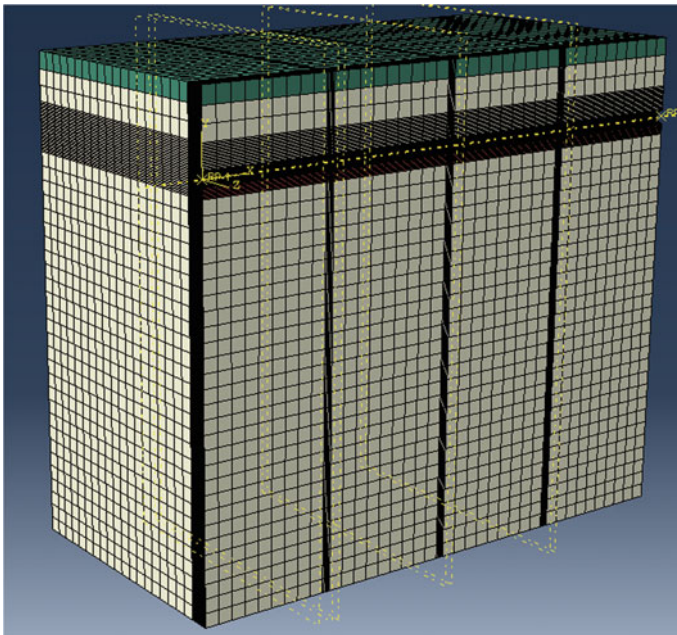


**Fig. 10** Meshing of the overall structure

Frictional contact was set at the intersection of roadbed and pipeline, tangentially as a penalty contact and normally as a hard contact. The friction coefficient of the pipe and soil contact surface was taken according to the following equation [28].

$$\mu = \frac{A}{H/D - B} + C \quad (1)$$

where, H is the embedment of the pipe from the mudline to the upper of pipe, A, B and C are fitting constants, depending on the undrained shear strength of the soil, which were taken as 0.756, 0.461 and 0.204 in this study [27], respectively.

### 3.2 Analysis and Discussion

On the established preface of road model, the impulse load measurement curve of the falling hammer bending instrument is used with an action area of 0.4 m × 0.2 m and a wheel spacing of 1.2 m, acting directly above and on both sides of S2, respectively, with reference to the literature [11, 12]. To make the simulation results of the road structure more realistic, the soil structure has been equilibrated before loading in this paper.

**Comparison of Mechanical Response of PVC Pipelines under Different Load Magnitudes.** The traffic load was applied to the road surface at the point directly above the pipe section S2, and the mechanical response of the buried pipeline with adhesive interface was studied under three different magnitude sizes of traffic load (0.6, 0.8 and 1.0 MPa). The longitudinal Mises stress distribution curves are shown in Fig. 11 for a point at each end of the pipe top to determine the path. To study the circumferential stress distribution of the pipe, the circumferential paths of the bell and the spigot at S2 were taken and the Mises stresses of the socket are analyzed under the action of traffic loads of three amplitudes. The stress comparison curves are shown in Fig. 12.

Due to the geometrical asymmetry of the socket structure, the Mises stresses at the top of the pipe in Fig. 11 were not symmetrical about the longitudinal centerline of the pipe and were highly discontinuous at the pipe joints. With the increase of the traffic load, the longitudinal Mises stresses of P2 and P3 pipe joints showed a significant increase, while the longitudinal Mises stresses of P1 and P4 pipe joints did not change significantly, which indicates that the influence of traffic load on the adhesive bonded joint was about 2 pipe joints (4 m).

As can be seen from Fig. 12, the stress distribution of the buried adhesive bonded joint of PVC pipe line bell and spigot had obvious peaks and valleys. The peaks of Mises stress distribution for the socket appeared at the top (0°) and the side (90°, 270°) of the pipe, and the valleys of Mises stress distribution are located at the shoulder (45°, 315°) and the bottom (360°) of the pipe. From the top to the bottom of the pipe, the Mises stress showed the distribution characteristics of first falling,

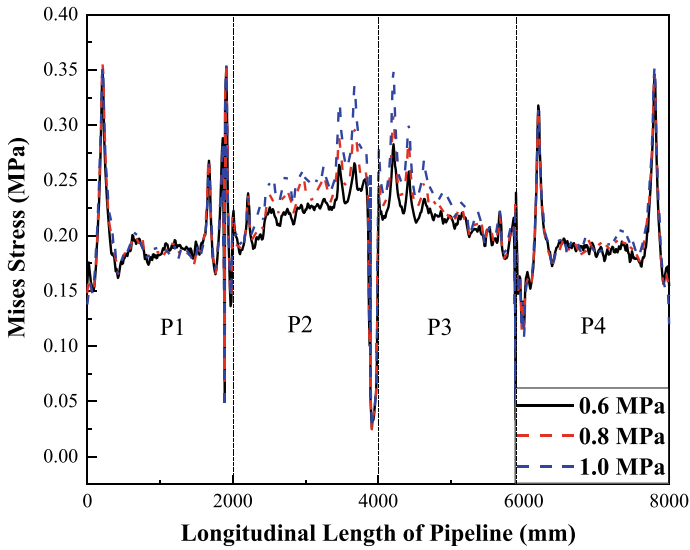


**Fig. 11** Comparison curve of Mises stress at the top of the pipeline under different magnitude of traffic load

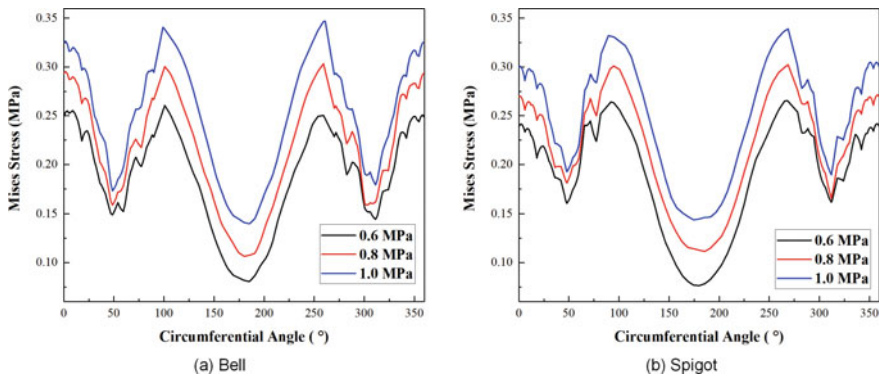


**Fig. 12** Mises stress comparison curves for bearing sockets in the circumferential direction under different traffic load magnitudes

then rising and then falling. The maximum Mises stress appeared at the side of the pipe ( $90^\circ$ ,  $270^\circ$ ) and the minimum Mises stress appeared at the bottom of the pipe ( $180^\circ$ ). Comparing the Mises stress distribution in the bell and the spigot, it can be found that the minimum and maximum Mises stresses in the spigot are smaller than those in the bell, but the minimum Mises stresses in the spigot are larger than those in the bell at the tube side ( $90^\circ$ ,  $270^\circ$ ), where the spigot is at the valley. In addition, with the increase of the traffic load amplitude, the circumferential Mises stress of the socket increased, and the effect of the Mises stress distribution law was especially

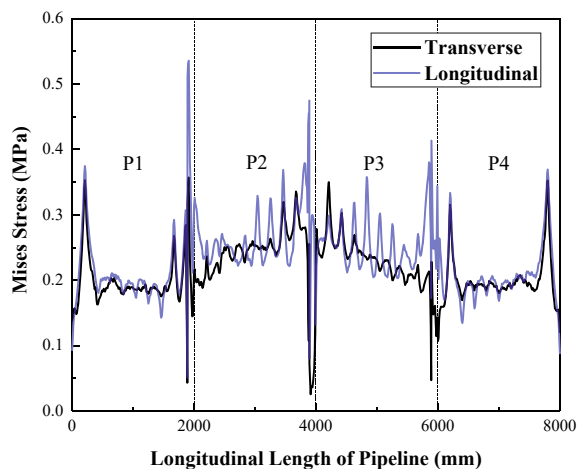
obvious for the lower part of the pipe ( $90^{\circ}$ – $270^{\circ}$ ), while the effect of the Mises stress distribution law was relatively small for the upper part of the pipe, especially the pipe shoulders.

**Comparison of Mechanical Response of PVC Pipelines under Different Traffic Direction.** The direction of the traffic load may be either perpendicular to the buried pipeline (transverse) or parallel to the buried pipeline (longitudinal). The traffic load in two different traffic directions is now applied to the road surface at the point directly above the pipe joint S2 to study the mechanical response of the buried pipeline with adhesive interface. The longitudinal Mises stress distribution curves are shown in Fig. 13 for a point at each end of the pipe top to determine the path. To study the stress distribution around the pipe perimeter, the circumferential paths of bell and spigot at S2 are taken, and the Mises stresses generated at bell and spigot by the traffic load under two traffic directions are analyzed. The stress comparison curves are shown in Fig. 14.

From Fig. 13, the direction of travel changed from transverse to longitudinal, the distribution pattern of Mises stress at the top of the pipe did not change significantly, but the magnitude of its stress increased significantly which was most obvious at the interface and smaller at the body of the pipe. This indicates that, under the same conditions, buried pipes laid along the road are more prone to rupture failure than buried PVC pipes with adhesive bonded joints across the road. In addition, the change in the direction of traffic did not significantly affect the Mises stresses at the top of the two pipe sections P1 and P4, which again indicates that the mechanical response of the traffic load on the buried pipeline is limited to the middle two pipe sections (4 m).

As can be seen from Fig. 14, the direction of travel had a greater effect on the circumferential dynamic response. When the direction of travel changes from transverse to longitudinal, the valley of the Mises stress distribution changed, and the

**Fig. 13** Comparative Mises stress curves at the top of the pipeline under the traffic load in different traffic directions



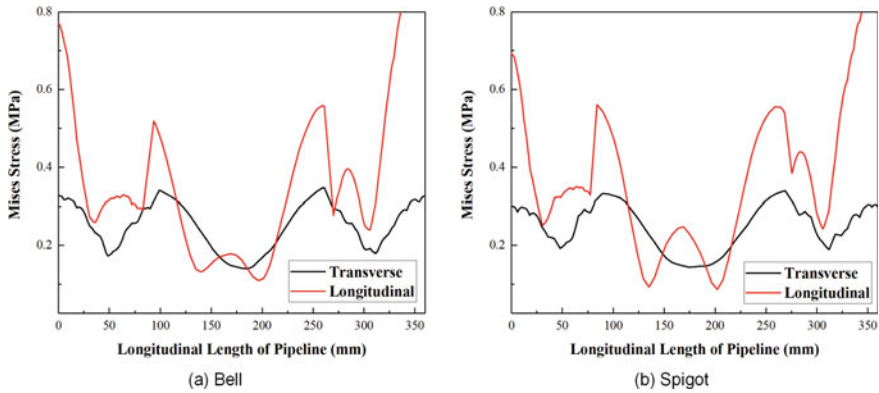


**Fig. 14** Mises stress comparison curves in the circumferential direction of the bearing socket under traffic loads in different directions of travel

shoulder ( $45^\circ$ ,  $315^\circ$ ) and the bottom ( $180^\circ$ ) are no longer the minima, but the minima fell symmetrically near the shoulder ( $30^\circ$ ,  $75^\circ$ ,  $285^\circ$ ,  $320^\circ$ ) and near the bottom ( $145^\circ$ ,  $215^\circ$ ). In addition, the change in the direction of travel caused the Mises stress in the upper part of the pipe to increase significantly, and the increase was much higher than that in the lower part of the pipe, which indicates that the Mises stress distribution pattern in the upper part of the pipe is more sensitive to the longitudinal direction of travel.

As can be seen from Fig. 13, the direction of travel has a greater effect on the circumferential dynamic response. When the direction of travel changes from transverse to longitudinal, the location of the valleys of the Mises stress distribution were relocated, and the number of both valleys and peaks both changed from three to six. The shoulders ( $45^\circ$ ,  $315^\circ$ ) and the bottom ( $180^\circ$ ) were no longer the minima, but the new minima fall symmetrically on both sides of the shoulders ( $30^\circ$ ,  $75^\circ$ ,  $285^\circ$ ,  $320^\circ$ ) and on both sides of the bottom ( $145^\circ$ ,  $215^\circ$ ), which makes the weakest point of the interface that the lowest value of the circumferential stress distribution of the interface, became the hips ( $145^\circ$ ,  $215^\circ$ ) of pipe. The Mises stress at the bottom of the pipe under the longitudinal direction of travel is higher than that under the transverse direction of travel. In addition, the change in the direction of travel caused a significant increase in the Mises stress in the upper part of the pipe, which is much higher than that in the lower part of the pipe, indicating that the Mises stress distribution pattern in the upper part of the pipe was more sensitive to the longitudinal direction of travel, which is opposite to the effect of the transverse direction of travel on the stress distribution pattern.

## 4 Conclusion

In this study, the axial mechanical performance and buried mechanical response of the adhesive bonded joint of PVC pipes were calculated numerically on basis of existing studies, the following conclusions were obtained.

1. The seismic performance of PVC pipe adhesive interface is poor, and the axial pullout displacement is very small, so it is difficult to resist the axial deformation under seismic damage like the flexible interface; the ultimate axial pullout force of adhesive interface is inversely proportional to the socket gap and proportional to the pipe diameter, while the influence of loading rate on the pullout force is limited and can be negligible.
2. Under the action of traffic load, the stress on the top and side of buried PVC adhesive bonded joint is obviously larger and prone to damage. And the maximum Mises stress by circumferential distribution of the bell is larger than that of the spigot, so bell is more susceptible to damage than the spigot in buried situations.
3. Different traffic directions have a greater influence on the mechanical response of the adhesive bonded joint. In the longitudinal traffic direction, the maximum circumferential Mises stress on the interface is significantly greater than that in the transverse traffic direction, and the location of the circumferential stress valley is relocated. The number of valleys is increased to 6 from 3, but it does not change the location of the circumferential stress Mises peak, so it does not change the location of damage accordingly.

## References

1. Sun SP, Han Y (2003) State-of-the-art of the research on lifeline earthquake engineering. *China Civ Eng J* (05):97–104
2. Wang Q, Guo MJ et al (2022) High performance PVC axial hollow wall pipes in urban drainage projects. *Water Wastewater Eng* 58(S1):406–411
3. Han Y, Li GC et al (2020) Experimental study on axial mechanical properties of pipeline under pseudo-static loading. *J Earthquake Eng Vibr* 40(05):44–51
4. Ren XZ, Han Y, Yang JC (2019) Experimental study on mechanical properties of ductile iron pipe flexible joint under eccentric tension. *J Henan Univ Urban Constr* 28(05):37–40
5. Zhong ZL, Wang SR et al (2019) Experimental study on mechanical properties of ductile iron pipeline rehabilitated by corrosion protection lining. *J Harbin Inst Technol* 51(06):141–147
6. CJJ 101-2016 (2016) Technical specification for buried plastic pipeline of water supply engineering
7. CJJ 143-2010: Technical specification for buried plastic pipeline of sewer engineering
8. Chen CG, Yang et al (2012) Experimental research on seismic capability of cast-iron pipe with rubber gasket joints. *J Earthquake Eng Eng Vibr* 32(03):104–108
9. Li GC, Ren XZ, Han Y (2020) Experimental study on mechanical properties of socket type flexible joint of pipeline under reciprocating load. *J Henan Univ Urban Constr* 29(01):29–33
10. Duan JF (2011) Experimental study on mechanical behavior of rubber gasketed joint with ductile cast iron pipe. Henan University of Technology

11. Wang FM, Fang HY et al (2018) Dynamic response analysis of drainage pipes with gasketed bell and spigot joints subjected to traffic loads. *Chin J Geotech Eng* 40(12):2274–2280
12. Wang FM, He H et al (2020) Study on mechanical response of the bell-and-spigot joints of pipeline under the coupling of traffic and running load. *J Zhengzhou Univ (Eng Sci)* 41(04):1–6
13. Zhai KJ, Fang HY et al (2020) Mechanical properties and failure mode simulation analysis of joints in PCCP. *China Water Wastewater* 36(20):10–18
14. Chen LP, Wang JS et al (2021) Study on joint leakage law of municipal concrete drainage pipeline. *Water Resour Hydropower Eng* 52(6):223–232
15. Zhang ZG, Fang L et al (2021) Influence analyses on force of gas pipeline with discontinuous joints induced by landslide on rainfall condition. *Chin J Geotech Eng* 1–10
16. Wu WY, Zhang TQ et al (2002) Calculation of longitudinal mechanics of flexible interface pipes under vertical load. *China Water Wastewater* (09):58–60
17. CJT 493-2016: High performance unplasticized poly (vinyl chloride) pipes and fittings for water supply
18. GB/T 10002.1-2006: Pipes and fittings made of unplasticized poly (vinylchloride) (PVC-U) for water supply—specifications
19. Guo S (2019) Methods and mechanisms of toughening of adhesively bonded joints. Tsinghua University
20. He X (2011) A review of finite element analysis of adhesively bonded joints. *Int J Adhes Adhes* 31(4):248–264
21. Camanho PP, Davila CG (2002) Mixed-mode decohesion finite elements for the simulation of delamination in composite materials. NASA/TM-2002–211737, pp 1–37
22. Camanho PP, Davila CG, De Moura MF (2003) Numerical simulation of mixed-mode progressive delamination in composite materials. *J Compos Mater* 37(16):1415–1438
23. Benzeggagh ML, Kenane M (1996) Measurement of mixed-mode delamination fracture toughness of unidirectional glass/epoxy composites with mixed-mode bending apparatus. *Compos Sci Technol* 56:439–449
24. GB/T 6329-1996 (1996) Adhesives-determination of tensile strength of butt joints
25. GB/T 33799-2017 (2017) Adhesives-determination of the bond strength of engineering-plastic joints
26. QB/T 2568-2002 (2002) Solvent cements for poly (vinyl Chloride) (PVC) plastic piping system
27. Fang H, Tan PL et al (2020) Numerical and experimental investigation of the effect of traffic load on the mechanical characteristics of HDPE double-wall corrugated pipe. *Appl Sci* 10(2):627
28. Wang J, Yang Z (2016) Axial friction response of full-scale pipes in soft clays. *Appl Ocean Res* 59:10–23